

Published in final edited form as:

*Mol Cancer Ther.* 2010 November ; 9(11): 2903–2913. doi:10.1158/1535-7163.MCT-10-0546.

## Adamantyl-substituted retinoid-related (ARR) molecules induce apoptosis in human acute myelogenous leukemia cells

Lulu Farhana<sup>1,\*</sup>, Marcia I Dawson<sup>3</sup>, Zebin Xia<sup>3,\*</sup>, Amro Aboukameel<sup>2,\*</sup>, Liping Xu<sup>1</sup>, Gang Liu<sup>3</sup>, Jayanta K Das<sup>1</sup>, James Hatfield<sup>4</sup>, Edi Levi<sup>4</sup>, Ramzi Mohammad<sup>2</sup>, and Joseph A Fontana<sup>1</sup>

<sup>1</sup> John D Dingell VA Medical Center, Department of Medicine, Karmanos Cancer Institute, Wayne State University, Detroit, MI

<sup>2</sup> Department of Medicine, Karmanos Cancer Institute, Wayne State University, Detroit, MI

<sup>3</sup> Sanford-Burnham Medical Research Institute, La Jolla, CA

<sup>4</sup> John D Dingell VA Medical Center, Pathology Service, Detroit, MI

### Abstract

The adamantyl-substituted retinoid-related compounds, 3-Cl-AHPC and AHP3 induce apoptosis *in vitro* and *in vivo* in a newly established human AML cell line, FFMA-AML and in the established TF(v-SRC) AML cell line. FFMA-AML and TF(v-SRC) cells displayed resistance to the standard retinoids- (including *trans* retinoic acid, 9 *cis* retinoic acid and the synthetic retinoid TTNPB) mediated apoptosis but sensitivity to 3-Cl-AHPC- and AHP3- mediated apoptosis *in vitro* and *in vivo* as documented by PARP cleavage and apoptosis TUNEL assay. 3-Cl-AHPC or AHP3 exposure *in vitro* resulted in decreased expression of the anti-apoptotic proteins (c-IAP1, XIAP) and phospho-Bad and activated the NF- $\kappa$ B canonical pathway. A significant prolongation of survival was observed in both NOD-SCID mice carrying FFMA-AML cells and treated with either 3-Cl-AHPC or AHP3 and SCID mice carrying TF(v-SRC) cells and treated with AHP3. We have previously shown that ARR bind to the orphan nuclear receptor small heterodimer partner (SHP) and that the expression of SHP is required for ARR-mediated apoptosis. Induced loss of SHP in these AML cells blocked 3-Cl-AHPC- and AHP3-mediated induction of apoptosis. These results support the further development of 3-Cl-AHPC and AHP3 as potential therapeutic agents in the treatment of AML patients.

### Keywords

3-Cl-AHPC; Leukemia; AML

### Introduction

Numerous advances based on recent molecular observations have been made in both the classification and prognosis of acute myelogenous leukemia (AML). While the inherent heterogeneous nature of AML was initially described using the French-American-British classification, the discovery of unique chromosomal translocations, gene amplification and mutations and their effects on prognosis and response to therapy has resulted in new and

\*These authors contributed equally to this work.

#### Disclosure of Potential Conflicts of Interest

No potential conflicts of interest were disclosed.

more clinically relevant classification systems (1–3). Despite these advances, the mainstay for AML treatment has remained chemotherapy. Targeted therapy has played a role in the treatment of selective AML subtypes. Treatment of acute promyelocytic leukemia (APL) with pharmacologic concentrations of *trans*-retinoic acid (tRA) results in 90% of the patients achieving a complete remission (4). The dramatic response of APL cells to high concentrations of tRA is due to the presence of a unique 15:17 reciprocal translocation resulting in the generation of a promyelocytic leukemia (PML)-retinoic acid nuclear receptor (RAR) $\alpha$  fusion product which displays increased binding to co-repressors in the presence of physiologic concentrations of tRA. This results in maturation arrest at the promyelocyte stage (5). Exposure of these cells to pharmacologic concentrations of tRA results in the disassociation of PML-RAR from the co-repressors, enhancing its binding by co-activators with the subsequent initiation of gene transcription. Unfortunately, tRA efficacy is restricted to APL with no activity demonstrated in the other AML subtypes. New targeted agents including fms-related tyrosine kinase receptor (FLT-3) and farnesyltransferase inhibitors are being evaluated as potential therapeutic modalities for the treatment of AML (6,7).

Adamantyl-substituted retinoid related (ARR) molecules are a unique class of compounds which have been found to induce apoptosis in a large number of tumor types many of which display resistance to classical retinoids (8–10). The precise mechanism(s) by which ARR<sub>s</sub> induce cell death is not clear. While 6-[3-(1-adamantyl)-4-hydroxyphenyl]-2-naphthalenecarboxylic acid (CD437/AHPN) was initially designed as a selective activator of RAR<sub>s</sub>  $\beta$  and  $\gamma$ , it has been found to inhibit cell growth and induce apoptosis in a variety of malignant cell types utilizing a RAR and retinoid  $\times$  receptor (RXR) independent mechanism (11–13). In addition, we have found that 4-[3-(1-adamantyl)-4-hydroxyphenyl]-3-chlorocinnamic acid (3-Cl-AHPC) which binds to RAR $\gamma$  (but does not activate RAR<sub>s</sub> or RXR<sub>s</sub>) is a potent inducer of apoptosis in AML cells *in vitro* (14). We have also reported that the novel nuclear receptor, small heterodimer partner (SHP, NR0B2) is involved in the induction of apoptosis by the ARR<sub>s</sub> (15).

In this report we demonstrate that 3-Cl-AHPC and its analog (*E*)-3-{2-[3-(1-adamantyl)-4-hydroxyphenyl]-5-pyrimidinyl}-2-propenoic acid (AHP3) inhibit the growth and induce apoptosis of the AML cells both *in vitro* and *in vivo*. In these studies, we used the TF(v-SRC) AML cell line and a human AML cell line FFMA-AML, which we had previously established from primary AML cells; both of these AML cell lines will grow *in vitro* and *in vivo* and are resistant to retinoid-mediated inhibition of cellular proliferation and induction of apoptosis, but are sensitive to the anti-proliferative and apoptotic effects of the ARR<sub>s</sub>. In addition, 3-Cl-AHPC- and AHP3-mediated apoptosis was accompanied by activation of the canonical NF- $\kappa$ B pathway, decreased expression of a number of anti-apoptotic proteins including the E-3 ligase c-IAP1 and required the expression of orphan receptor protein SHP.

## Materials and Methods

### ARR<sub>s</sub>

3-Cl-AHPC was synthesized as previously described (14). AHP3 was synthesized as described in supplemental information.

### Retinoids and antibodies

RAR-selective retinoids *trans*-RA, RAR and RXR-selective 9-*cis*-RA and RAR selective (*E*)-4-[2-(5,6,7,8-tetrahydro-5,5,8,8-tetramethyl-2-naphthyl)propenyl]benzoic acid (TTNPB) were synthesized in the lab. ARR<sub>s</sub> and retinoids were solubilized in dimethylsulfoxide prior to addition to cells. The maximum concentration of vehicle per culture was 0.1%. RPMI-1640 medium, fetal bovine serum (FBS) and Trizol reagent were purchased from

Invitrogen (Grand Island, NY). Anti-XIAP, anti-NF $\kappa$ Bp65, anti-IKK $\alpha$ /IKK $\beta$  and anti-SHP antibodies were obtained from Santa Cruz Biotechnology (Santa Cruz, CA). Anti-phospho-NF $\kappa$ Bp65 (Ser276), phospho-IKK $\alpha$  (ser180)/IKK $\beta$  (Ser181), phospho-Bad, anti-caspase-3 and active cleaved caspase-3 antibodies were purchased from Cell Signaling (Bellerica, MA), while anti-c-IAP1 antibody and  $\alpha$ -tubulin were obtained from (R & D Systems Inc., Minneapolis, MN) and Oncogene Research Products (Boston, MA), respectively.

**Acute myelogenous leukemia cells**—The FFMA-AML cells were obtained from a patient with a diagnosis of AML as indicated by the immunophenotyping described in Supplementary file Table 1. This patient was refractory to the chemotherapy regimens consisting of cytosine arabinoside administered with daunomycin as well as high dose cytosine arabinoside. Peripheral blood samples were obtained from the patient under the guidelines of a Wayne State University Institutional Review Board approved protocol. The leukemic blasts were isolated by Ficoll- hypaque density gradient. The isolated leukemic cells (representing >99% of the cells) were subsequently cultured in RPMI-1640 supplemented with 10% heat inactivated fetal bovine serum and growth factors interleukin 3 (IL-3), granulocyte-colony stimulating factor (G-CSF), granulocyte/macrophage colony-stimulating factor (GM-CSF) and stem cell factor (SCF) as we have previously reported (14). After the cell line became established, cells were maintained in RPMI-1640 medium supplemented with 10% FBS and 500  $\mu$ g/ml gentamycin (14). The establishment of the TF(v-SRC) cell line has been previously described (16). TF(v-SRC) cells were grown in RPMI-1640 supplemented with 10% heat inactivated fetal bovine serum.

### Western blots and RT-PCR

Western blots, RNA preparation and RT-PCR were performed as we have previously described (17).

### Apoptosis

Apoptosis of cells was determined by (1) acridine orange and ethidium bromide-staining to determine the percentage of cells with nuclear fragmentation and chromatin condensation as previously described (17), and (2) flow cytometry analysis of Annexin V-FITC binding together with propidium iodide staining (Annexin V-FITC apoptosis Detection kit 1, BD Biosciences, San Diego, CA). Data acquisition was performed using a FACS Calibur flow cytometer (BD) and analyzed with CellQuest software (BD Biosciences, CA).

### shRNA SHP knockdown

shRNA SHP retroviral expression vectors were prepared as we have described (18). FFMA-AML and TF(v-SRC) cell lines were transiently transfected with retroviral shRNA-SHP plasmids either for 48 or 72 h. SHP protein expression was assessed using Western blots after 72 h infection with shRNA SHP retroviral expression vector in the FFMA-AML and TF(v-SRC) cells. Anti-SHP antibodies were obtained from MBL International Corporation, (Woburn MA) and Santa Cruz Biotechnology, (Santa Cruz, CA). Effect of SHP knockdown on ARR induction of apoptosis in cells was assessed 48 h following infection with shRNA SHP expression vectors. Apoptosis was determined using an Annexin V-FITC apoptosis detection kit described above.

### *In vivo* studies

All *in vivo* studies were conducted in accordance with Wayne State University (WSU) approved animal care and ethics committee guidelines and procedures. Non-obese diabetic severe combined immunodeficiency (NOD-SCID) and ICR-SCID mice were obtained from

Jackson Laboratories (Bar Harbor, Maine) and Taconic Farms (Germantown, New York), respectively.

#### A) FFMA-AML and TF(v-SRC) systemic model

NOD-SCID and ICR-SCID mice (4 to 5 weeks old) were injected intravenously with either FFMA-AML or TF(v-SRC) cells. Treatment with vehicle, 3-Cl-AHPC or AHP3 was instituted the following day. If symptoms such as diarrhea, dehydration, weight loss, ascites, paralysis or general weakness became evident, mice were euthanized.

#### B) TF(v-SRC) subcutaneous mouse model

ICR-SCID mice were bilaterally trocared subcutaneously with TF(v-SRC) tumor fragments. Animals with equal tumor weights were assigned to three experimental groups as we have previously described (26): Group 1) control (vehicle treated), Group 2) subcutaneous injections of AHP3 and Group 3) intravenous injections of AHP3. The percent increase in the host life span (%ILS) of the FFMA-AML and TF(v-SRC) bearing mice was calculated by subtracting the median day of death of the drug-treated AML cell line-bearing mice from the median day of death of the vehicle-treated AML cell line-bearing mice divided by the median day of death of the AML cell line-bearing vehicle treated mice.

To determine the efficacy of the 3-Cl-AHPC and AHP3, survival distribution of the 3-Cl-AHPC or AHP3 treated (T) or vehicle (C) groups were compared using the log-rank test. Survival was characterized as the duration of the animal's life span beginning 24 h after the initiation of the xenograft until an observed event (euthanasia or death). A p-value of less than 5% ( $p < 0.05$ ) was considered statistically significant.

***In Situ Cell Death Detection and immunohistochemistry***—The TUNEL assay was performed using the *In Situ Cell Death Detection* kit, POD (Roche-Applied-Science, Mannheim, Germany) according to the manufacturer's instructions. Frozen tumor samples were fixed for 24 hrs in 10 % formalin buffered-saline, then dehydrated and embedded 4  $\mu$ m thick sections in paraffin. The tissue sections were deparaffinized and rehydrated, then tissues sections were incubated with proteinase K solution (10–20  $\mu$ g/ml) for 30 min. Tissues were then rinsed twice in PBS and reacted with 50  $\mu$ l of the TUNEL reaction mixture at room temperature for 60 min in a dark, humidified chamber. Sections were again rinsed in PBS and incubated for 30 min with 50  $\mu$ l of the Converter-POD (Roche-Applied-Science) and followed by 3-amino-9-ethylcarbazole (AEC). Sections were then counterstained with hematoxylin. As negative controls, corresponding sections were treated in the same way without terminal deoxynucleotidyl transferase. Under light microscopy, the number of TUNEL-positive cells were counted and expressed as a percentage of the total number of cells present in that field.

For immunohistochemistry, paraffin-embedded sections were deparaffinized, rehydrated, and antigen unmasking was performed by immersing the slides in boiling 0.01M citrate buffer for 15 min. Endogenous peroxidase activity was blocked with 3.0% hydrogen peroxide for 30 min. Tissue sections were incubated overnight at 4°C with cleaved-PARP (Asp214) antibody (Cell signaling, Bellerica, MA) diluted in 1:25 dilution, then incubated with biotinylated secondary antibody. We used an avidin-biotinylated horseradish peroxidase complex (Vectastain ABC Reagent; Vector Laboratories) with AEC (BioGenex Laboratories Inc, San Ramon, CA) as a chromogen, for visualization of the immunoreaction. Slides were counterstained with hematoxylin. Primary antibody was omitted for negative control.

## Results

### Structures of 3-Cl AHPC and AHP3

The chemical structures of ARRs 3-Cl-AHPC and AHP3 are outlined in Fig. 1A. Synthesis and characterization of 3-Cl-AHPC has been previously described (14) while that of AHP3 is described in Materials and Methods.

### 3-Cl AHPC- and AHP3-induced apoptosis and inhibition of proliferation in FFMA-AML cells

The proliferation of TF(v-SRC) and FFMA-AML cells was inhibited by exposure to 3-Cl-AHPC and AHP3 (Supplementary Fig. S1A and B). 3-Cl-AHPC and AHP3 induction of apoptosis in FFMA-AML and TF(v-SRC) cells was examined by assessing the number of cells demonstrating nuclear fragmentation and chromatin condensation (Fig. 1B, C and D). Cells were grown in the presence and absence of increasing concentrations of either 3-Cl-AHPC or AHP3 for 96 h or were exposed to 1  $\mu$ M 3-Cl-AHPC or AHP3 from 0–96 hr. There was a progressive increase in 3-Cl-AHPC- and AHP3- mediated apoptosis in both FFMA-AML and TF(v-SRC) cells with increasing concentrations of the compounds and over time (Fig. 1B and C). Compared to FFMA-AML cells, TF(v-SRC) cells displayed less sensitivity to both 3-Cl-AHPC and AHP3 (ED50 of 0.75  $\mu$ M) whereas FFMA-AML cells displayed ED50s of 0.32  $\mu$ M and 0.37  $\mu$ M to AHP3 and 3-Cl-AHPC, respectively (Fig. 1B and C). Previous studies have demonstrated that acute promyelocytic leukemia (APL) cells undergo apoptosis in the presence of tRA, 9-*cis* RA and the RAR $\alpha$  selective retinoid, TTNPB, through their ability to bind to the PML-RAR fusion protein (5). Therefore, we tested the sensitivity of FFMA-AML and TF(v-SRC) cells to apoptosis induced by tRA, 9-*cis* RA and TTNPB (Fig. 1D). The addition of either tRA, 9-*cis* RA or TTNPB to the FFMA-AML cells resulted in an approximately 10 to 20% of the cells exhibiting apoptosis (compared to those treated with the vehicle) while the addition of 3-Cl-AHPC induced apoptosis in 80% of the cells (Fig. 1D). TF(v-SRC) cells were resistant to apoptosis induction by these compounds with 9-*cis*-RA, tRA or TTNPB exposure resulting in no real increase in apoptosis (Fig. 1D).

To further document 3-Cl-AHPC and AHP3-mediated apoptosis in the FFMA-AML and TF(v-SRC) cells, the percentage of cells undergoing apoptosis was assessed using flow cytometry. There was a progressive increase in the percentage of apoptotic cells (Fig. 2A and B). Previous studies have shown that (CD437/AHPN) and 3-Cl-AHPC induce apoptosis in variety of malignant cells through a caspase-dependent processes (9, 18). Thus we examined whether apoptosis was associated with the activation of caspase-3 in AML cells. 3-Cl-AHPC and AHP3 increased caspase 3 activity in the treated AML cells (Fig. 2C) and induced caspase-3 activation as indicated by the generation of the catalytically active 17 kDa cleaved caspase-3 protein (Fig. 2D).

### AHP3 inhibits expression of anti-apoptotic protein X-linked inhibitor of apoptosis protein (XIAP), cellular inhibitor of apoptosis 1 (c-IAP1) and phospho-Bad

The proteins c-IAP1, c-IAP2 and XIAP bind caspases resulting in inhibition of caspase activity (19). In addition, c-IAP1 and c-IAP2 possess E3-ligase activity targeting protein destruction through the proteasome pathway and play an important role in NF- $\kappa$ B activation (19). The Bcl-2 family member Bad enhances apoptosis and is inactivated through phosphorylation and the generation of phosphorylated Bad (20). To assess AHP3 modulation of anti-apoptotic protein expression during the induction of apoptosis in AML cells, we assessed the expression of XIAP, c-IAP1 and phospho-Bad as well as cleavage of the DNA-damage repair poly (ADP-ribose) polymerase (PARP) following exposure of AML cells to AHP3 (Fig. 3A). Exposure of FFMA-AML and TF(v-SRC) cells to AHP3 *in vitro* resulted in a 70 to 80% decreased expression of the anti-apoptotic proteins XIAP and

c-IAP-1, and phospho-Bad (Fig. 3A, Supplementary Fig. S1C); In addition, PARP cleavage was accompanied the decrease in c-IAP1, XIAP and phospho-Bad levels, further documenting initiation of apoptosis induced by AHP 3 in AML cells (Figures 3A and Supplementary Fig. S1D).

Activation of the NF- $\kappa$ B canonical pathway requires I $\kappa$ B kinase (IKK) $\beta$  activation, phosphorylation of I $\kappa$ B $\alpha$  which sequesters the NF- $\kappa$ B p65 subunit in the cytoplasm, followed by phosphorylated I $\kappa$ B $\alpha$  destruction through the proteasome pathway and the release and nuclear translocation of p65. Exposure of FFMA-AML and TF(v-SRC) cells to AHP3 or 3-Cl-AHPC resulted in a decrease in I $\kappa$ B $\alpha$  levels (Fig. 3B) and increased nuclear phospho-p65 (Ser276) levels (Fig. 3C), indicating activation of the NF- $\kappa$ B canonical pathway. Phosphorylation of the activation loops of IKK $\alpha$  and IKK $\beta$  has been associated with their conformational change and IKK kinase activation (21,22). Thus, we assessed whether exposure of the FFMA-AML and TF(v-SRC) to AHP3 resulted in IKK $\alpha$  and/or IKK $\beta$  phosphorylation and thus activation of the canonical and/or noncanonical NF- $\kappa$ B pathways. Exposure of FFMA-AML and TF(v-SRC) to AHP3 resulted in enhanced phosphorylation of both IKK $\alpha$  and IKK $\beta$ . FFMA-AML cells exposed to AHP3 exhibited increased IKK $\alpha$  phosphorylation at 6 hr (1.6-fold) and at 24 hr (1.2-fold) with no further increase at 48h (Fig. 3D and Supplementary Fig. S2), while IKK $\beta$  phosphorylation was increased at 6 h (1.2 fold) with no further increase noted at 24 h and 48 h in these cells (Fig. 3D and Supplementary Fig. S2). Exposure of TF(v-SRC) cells to AHP3 resulted in a steady increase in IKK $\alpha$  phosphorylation at 6 h (1.6 fold), 24 h (1.6 fold) and 48 h (1.9 fold) as well as a steady increase in IKK $\beta$  phosphorylation from 6 h (1.7 fold) to 24 h (1.8 fold) and 48 h (2.1 fold) (Fig. 3D and Supplementary Fig. S2). The compound JSH-23, selectively blocks nuclear translocation of the NF- $\kappa$ Bp65/Rel A subunit and its heterodimerization with p50 and is associated transcriptional activation (23). We used JSH-23 to examine its effect on AHP3 and 3-Cl-AHPC-mediated apoptosis in TF(v-SRC) cells. While JSH-23 induced apoptosis in approximately 20% of the cells alone, it inhibited 3-Cl-AHPC and AHP3-mediated apoptosis in TF(v-SRC) cells indicating that activation of the NF- $\kappa$ B canonical pathway is required for apoptosis induction by these compounds (Fig. 3D, right panel).

### **Loss of SHP expression inhibits AHP3 inhibition of proliferation and the induction of apoptosis in TF(v-SRC) cells**

The orphan nuclear receptor SHP has been found to bind to numerous nuclear receptors resulting in the inhibition of their transcriptional activation (24,25). SHP has been found to be expressed in a number of tissues including the human HL-60 AML cell line (25). We demonstrated that SHP is expressed in the human FFMA-AML and TF(v-SRC) cells using RT-PCR (Supplementary Fig. S3A). Knock-down of SHP expression in the TF(v-SRC) cells was achieved utilizing shRNA directed at SHP (Supplementary Fig. S3B). Loss of SHP expression resulted in the inhibition of 3-Cl-AHPC mediated apoptosis as indicated by annexin V-FITC and propidium iodide staining (Fig. 4A and B). The loss of SHP expression also blocked 3-Cl-AHPC and AHP3-mediated inhibition of TF(v-SRC) and FFMA-AML proliferation (Fig. 4C). Loss of SHP expression had no effect on the proliferation of MDA-MB-468, MEF or KG-1 cells as reported previously (18).

### **3-Cl-AHPC and AHP3 inhibition of FFMA-AML growth in NOD-SCID mice**

3-Cl-AHPC and AHP3 inhibition of FFMA-AML cell growth in NOD-SCID mice was determined. NOD-SCID mice were randomly assigned to two groups of eight mice and were injected with 1 million cells through the tail vein. The mice then received either vehicle or 3-Cl-AHPC (30 mg/kg) administered intravenously twice daily for 4 days. 3-Cl-AHPC treatment of the NOD-SCID mice resulted in a significant (p value 0.0001) increase in the length of survival (25%) compared to mice treated with vehicle only (Fig. 5A). Similar

results were obtained when 3-Cl-AHPC was given through an intraperitoneal route using the same dosage of 3-Cl-AHPC and treatment schedule (Fig. 5A, right panel). Treatment of the mice with 3-Cl-AHPC was associated with toxicity including weight loss ( $16.3\% \pm 17\%$ ) and decreased physical activity. Similarly, mice were treated with AHP3, at doses of either 5.0 mg/kg or 7.5 mg/kg administered twice a day for 4 days. Although not resulting in a relevant antitumor effect, this treatment did result in a significant increase in survival time ( $p=0.0002$ ) compared to that in mice treated with vehicle alone (ILS 26%) (Fig. 5B). In contrast to 3-Cl-AHPC, treatment with AHP3 therapy was extremely well tolerated and no toxicity was evident (no weight loss and no lessening of physical activity).

### AHP3 inhibition of resistant TF(v-SRC) cell growth in SCID mice

We next assessed the ability of AHP3 to inhibit the growth of TF(v-SRC) cells in SCID mice. SCID mice were injected with 10 million TF(v-SRC) cells and the mice treated intravenously with AHP3 (20 mg/kg) or vehicle every other day for a total of 15 doses. Treatment with AHP3 resulted in a marked increase in the length of survival with no evidence of leukemia in 87 % of the treated mice (Fig. 5C). TF(v-SRC) cell growth in the SCID mice was documented by flow cytometry. Flow cytometric analysis of lymph node or tumor samples specimens obtained from the mice treated with vehicle revealed the presence of TF(v-SRC) cells exhibiting CD45, CD13, CD34, CD33, CD36 and CD40 expression in the lymph nodes and in tumor specimens (Supplementary file Table 2); no malignant cells were identified in the AHP3- treated surviving mice. Compared to vehicle treated mice, AHP3 treated mice did not show evidence of toxicity such as weight loss (Fig. 5C, right panel) or evidence of diarrhea, dehydration, scruffy coat or decreased physical activity.

### AHP3 inhibits the growth of palpable TF(v-SRC) tumors

The ability of AHP3 to inhibit the growth of palpable TF(v-SRC) tumors was also examined. TF(v-SRC) cells were trochared subcutaneously in SCID mice and cells were allowed to form palpable tumors as described in Materials and Methods. When the palpable tumors reached a size of 100 mg, mice were divided into two groups of eight mice each and received either vehicle or AHP3 (Fig. 5D). AHP3 was given either subcutaneously (at a remote site from the palpable tumor) or intravenously, at a dose of 20 mg/kg every other day for 4 doses. Control mice received vehicle intravenously. AHP3 treatment given either intravenously or subcutaneously at a distant site from the tumor resulted in an approximate 50 % reduction in TF(v-SRC) growth (Fig. 5D and 6A). In addition, AHP3 treatment of the mice resulted in the induction of apoptosis in the tumors as documented by immunohistochemistry staining utilizing the apoptosis TUNEL assay as well as PARP cleavage (Fig. 6B, C, and D).

## DISCUSSION

We have previously demonstrated that ARRs are potent inducers of apoptosis in leukemia cells (11). AHPN induced apoptosis *in vitro* in the HL-60 and HL-60R human AML cells with the latter expressing a deletion in the RAR $\alpha$  and thus displaying resistance to retinoid-mediated differentiation and apoptosis (11). In addition, we have demonstrated that exposure of AHPN to human primary CLL cells in culture resulted in apoptosis in CLL cells (26). While tRA-induced apoptosis is restricted to APL cells, ARRs do induce apoptosis in all categories of AML cells grown in culture (14). Human primary AML cells, which display resistance to tRA-mediated apoptosis, are exquisitely sensitive to 3-Cl-AHPC-mediated apoptosis *in vitro* with greater than 80% of the cells undergoing apoptosis after a 48 h incubation (14). In addition, incubation of these cells with 3-Cl-AHPC resulted in activation of the p38, ERK and JNK kinases(14). Similar ARR activation of the Jun, ERK, and p38

MAPP have been described by a number of investigators (27,28). The role(s) of these kinases in ARR-mediated apoptosis is unclear.

Here we show that 3-Cl-AHPC and AHP3 induce apoptosis in human AML cells *in vivo* as well as *in vitro*. Exposure of FFMA-AML as well as TF(v-SRC) cells to these compounds *in vitro* resulted in the induction of apoptosis while these cells were resistance to apoptosis induced by *t*RA, 9-*cis*RA and the RAR $\alpha$  selective TTNPB. Apoptosis was preceded by decreased expression of the anti-apoptotic proteins XIAP, c-IAP1 and phospho-Bad. 3-Cl-AHPC and AHP3 induced apoptosis TF(v-SRC) was dependent on the expression of the orphan nuclear receptor SHP and is similar to what we have as demonstrated in other malignant cell types (15).

AHP3 and 3-Cl-AHPC-induced apoptosis in the FFMA-AML and TF(v-SRC) cells was also preceded by the activation of the NF- $\kappa$ B canonical pathway. NF- $\kappa$ B activation has been demonstrated to inhibit apoptosis in a number of systems (17,29). Exposure of breast or prostate carcinoma cells to CD437/AHPN or 3-Cl-AHPC resulted in NF- $\kappa$ B activation (17,29). Inhibition of NF- $\kappa$ B signaling with a dominant negative I $\kappa$ B $\alpha$ , knockout of p65 or helenalin, a specific inhibitor of p65 translocation to the nucleus, inhibited CD437/AHPN and 3-Cl-AHPC-mediated NF- $\kappa$ B activation and apoptosis in these cells (17). Numerous studies have now demonstrated that NF- $\kappa$ B activation can also play a major role in the initiation apoptosis (17,29,30). The NF- $\kappa$ B activated genes which play important roles in 3-Cl-AHPC/AHP3 mediated apoptosis are now under investigation.

3-Cl-AHPC or AHP3 treatment of NOD-SCID mice injected with FFMA-AML cells resulted in significantly prolonged survival. FFMA-AML bearing mice treated with vehicle, 3-Cl-AHPC or AHP3 eventually developed paralysis requiring that they be euthanized as stipulated by Wayne State University animal care guidelines. The explanation for the development of paralysis FFMA-AML bearing mice is not clear but is under study. AHP3 treatment of SCID mice injected with TF(v-SRC) cells cured 87 % of the mice bearing these AML cells; this was associated with minimal to no toxicity to the mice. Thus, AHP3 and 3-Cl-AHPC demonstrated significant efficacy in inhibiting the growth of the AML cells both *in vitro* and *in vivo*.

The *in vitro* and *in vivo* mechanism(s) involved by which the ARRs induce apoptosis in the AML cells are still not clear. We and others have previously demonstrated that retinoic acid nuclear receptors and retinoic acid  $\times$  receptors are not involved despite reports that both AHPN and related ARRs can activate one or more RAR subtypes (8,9). A number of potential mechanisms by which the ARRs may induce apoptosis, have been suggested (31). Activation of the p38 and the c-Jun-NH2-kinases, inactivation of the MKP-1 phosphatase allowing for JNK activation and mobilization of TR3 from its nuclear localization to mitochondria with its binding to Bcl-2 have all been implicated as important mechanisms by which the ARRs induce apoptosis in malignant cells (31). We have recently found that SHP expression as well as that of Sin3A is essential for ARR-mediated apoptosis in a variety of cell types (15); knockdown or knockout of either SHP or Sin3A resulted in the inhibition of ARR-mediated apoptosis (15). The importance of SHP in ARR-mediated apoptosis is further supported by our observation that the loss of SHP expression in TF(v-SRC) cells inhibited ARR-mediated apoptosis. In addition, we have found that the ARRs specifically bind to SHP (15). SHP functions primarily as a repressor of gene expression. This is mediated by a number of nuclear receptors including the thyroid hormone receptor, retinoic acid receptor, retinoid  $\times$  receptor, estrogen receptor, glucocorticoid receptor and hepatocyte nuclear receptor -4. SHP has been demonstrated to be an activator of NF- $\kappa$ B- and peroxisome proliferator-activated receptor gamma-mediated transcription/gene activation (32,33). He et al(34) have recently found that SHP functions as a tumor suppressor in the



development of hepatocellular carcinoma. Furthermore, SHP appears to negatively regulate the proliferation of these cells through its ability to down-regulate cyclin D1 expression (35). We have also found that ARR-activation of NF $\kappa$ B is essential for ARR-mediated apoptosis (17). Down regulation of SHP expression has been shown to block ARR-mediated activation of NF- $\kappa$ B as well as ARR-mediated apoptosis (18). Interestingly, Bruserud et al (36) described high levels of NF- $\kappa$ B p65 in AML cells, which were felt to play a role in the increased transcription of a variety of cytokines resulting in enhanced cellular proliferation and perhaps resistance to therapy. The fact that ARR- induced apoptosis requires the activation of NF- $\kappa$ B in AML cells would imply that it is not simply NF- $\kappa$ B activation which is important but the environment in which NF- $\kappa$ B activation takes place and which specific genes are activated.

The Sin3A protein serves as a scaffold protein which through its four highly conserved but imperfect repeats, the paired amphipathic helix (PAH) domains, is capable of binding a variety of proteins (37–40). These include a number of important nuclear transcription factors such as p53 and MAD (37–40). 3-Cl-AHPC treated KG-1 AML cells resulted in the binding of ARR to SHP and the subsequent binding of SHP/ARR to the Sin3A complex; this association between SHP/ARR and the Sin3A complex results in the modification of the Sin3A complex and enhancement of its associated HDAC-1, -2 activity (18).

In this report we have demonstrated that the ARRs display significant efficacy in the *in vivo* treatment of mice bearing AML and resulted in the prolongation of their survival. In addition, treatment of SCID mice bearing TF(v-SRC) cells with AHP3 resulted in cure of 87% of the mice. We are now in the process of further delineating the role of SHP and ARR binding to SHP in ARR-mediated apoptosis as well as the synthesis of ARR analogs which will show greater efficacy, minimal toxicity and have better bioavailability.

## Supplementary Material

Refer to Web version on PubMed Central for supplementary material.

## Acknowledgments

We thank Dr. James McCubrey, East Carolina University for the gift of the TF(v-SRC) cell line.

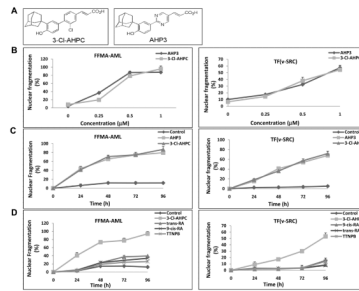
Financial Support: This work was supported by Veterans Affairs Merit Review Grant (JAF, MID) and NCI grants (JAF, MID); LF (NIH), MID (NIH), AA(NIH), LX (NIH), JKD (VA), RM (NIH) and JAF (NIH, VA).

## References

1. Byrd JC, Mrozek K, Dodge RK, et al. Pretreatment cytogenetic abnormalities are predictive of induction success, cumulative incidence of relapse, and overall survival in adult patients with de novo acute myeloid leukemia; results from Cancer and Leukemia Group B (CALGB 8461). *Blood*. 2002; 100:4325–4336. [PubMed: 12393746]
2. Grimwade D, Walker H, Harrison G, et al. The predictive value of hierarchical cytogenetic classification in older adults with acute myeloid leukemia (AML) analysis of 1065 patients entered into United Kingdom Medical Research Council AML 11 trial. *Blood*. 2001; 98:1312–1320. [PubMed: 11520776]
3. Mrozek K, Heerema NA, Bloomfield CD. Cytogenetics in acute leukemia. *Blood Rev*. 2004; 18:115–136. [PubMed: 15010150]
4. Warrell RP, Frankel SR, Miller WH, et al. Differentiation therapy of acute promyelocytic leukemia with tretinoin (all-trans-retinoic acid). *N Eng J Med*. 1991; 324:1385–1393.
5. Melnick A, Licht JD. Deconstructing a disease: RAR $\alpha$ , its fusion partners and their roles in the pathogenesis of acute promyelocytic leukemia. *Blood*. 1999; 93:3167–3215. [PubMed: 10233871]

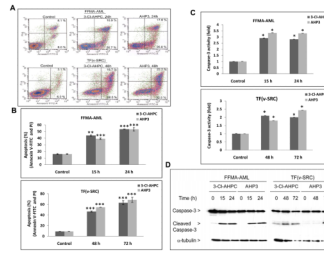
6. Burnett AK, Mohite U. Treatment of older patients with acute myeloid leukemia-new agents. *Semin Hematol.* 2006; 43:96–106. [PubMed: 16616043]
7. Meshinchi S, Appelbaum FR. Structural and alterations of FLT3 in acute myeloid leukemia. *Clin Cancer Res.* 2009; 15:4263–4269. [PubMed: 19549778]
8. Schadendorf D, Kern MA, Artuc M, et al. Treatment of melanoma cells with the synthetic retinoid CD437 induces apoptosis via activation of AP-1 in vitro, and causes growth inhibition in xenografts in vivo. *J Cell Biol.* 1996; 135:1889–1898. [PubMed: 8991099]
9. Mologni L, Ponzanelli I, Brescianni F, et al. The novel synthetic retinoid 6-[3-adamantyl-4-hydroxyphenyl]-2-naphthalene carboxylic acid (CD437) causes apoptosis in acute promyelocytic leukemia cells through rapid activation of caspases. *Blood.* 1999; 93:1045–1061. [PubMed: 9920855]
10. Garattini E, Parrella, Diomede L, et al. ST1926, a novel and orally active retinoid-related molecule inducing apoptosis in myeloid leukemia cells: modulation of intracellular calcium homeostasis. *Blood.* 2004; 103:194–207. [PubMed: 12958071]
11. Hsu CA, Rishi AK, Su-Li X, et al. Retinoid induced apoptosis in leukemia cells through a retinoic acid nuclear receptor-independent pathway. *Blood.* 1997; 89:4470–4479. [PubMed: 9192771]
12. Sun SY, Yue P, Chandraratna RA, Tesfaigzi Y, Hong WK, Lotan R. Dual mechanisms of action of the retinoid CD437: nuclear retinoic acid receptor-mediated suppression of squamous differentiation and receptor-independent induction of apoptosis in UMSCC22B human head and neck squamous carcinoma cells. *Mol Pharmacol.* 2000; 58:508–514. [PubMed: 10953043]
13. Parella E, Gianni M, Fratelli M, et al. Antitumor activity of the retinoid molecules (E)-3-(4'-hydroxy-3'-adamantylbiphenyl)acrylic acid (ST1926) and 6-[3-(adamantyl)-4- hydroxyphenyl]-2-naphthalenecarboxylic acid (CD437) in F9 teratocarcinoma: Role of retinoic acid receptor  $\gamma$  and retinoid-independent pathways. *Mol Pharmacol.* 2006; 70:909–924. [PubMed: 16788091]
14. Zhang Y, Dawson MI, Ning Y, et al. Induction of apoptosis in retinoid-refractory acute myelogenous leukemia by a novel AHPN analog. *Blood.* 2003; 102:3743–3752. [PubMed: 12893763]
15. Farhana L, Dawson MI, Leid M, et al. Adamantyl-substituted molecules bind SHP and modulate the Sin3A repressor. *Cancer Res.* 2007; 67:318–325. [PubMed: 17210713]
16. Black JH, McCubrey JA, Willingham MC, Ramage J, Hogge DE, Frankel AE. Diphtheria toxin-interleukin-3 fusion protein (DT<sub>388</sub>IL3) prolongs disease-free survival of leukemic immunocompromised mice. *Leukemia.* 2003; 17:155–159. [PubMed: 12529673]
17. Farhana L, Dawson MI, Fontana JA. Apoptosis induction by a novel retinoid-related molecule requires Nuclear Factor- $\kappa$ B activation. *Cancer Res.* 2006; 65:4909–4917. [PubMed: 15930313]
18. Farhana L, Dawson MI, Dannenberg JH, Xu L, Fontana JA. SHP and Sin3A expression are essential for adamantyl-substituted retinoid related molecules-mediated NF- $\kappa$ B activation, c-Fos/c-Jun expression and cellular apoptosis. *Mol Cancer Ther.* 2009; 8:1625–1635. [PubMed: 19509248]
19. Jin H-S, Lee D-H, Kim D-H, et al. cIAP1, cIAP2, and XIAP act cooperatively via nonredundant pathways to regulate genotoxic stress-induced nuclear factor- $\kappa$ B activation. *Cancer Res.* 2009; 69:1782–1701. [PubMed: 19223549]
20. Eisenmann KM, VanBrocklin MW, Staffend NA, Kitchen SM, Koo HM. Mitogen-activated protein kinase pathway-dependent tumor specific survival signaling in melanoma cells through inactivation of the proapoptotic protein bad. *Cancer Res.* 2003; 63:8330–8337. [PubMed: 14678993]
21. Delhase M, Hayakawa M, Chen Y, Karin M. Positive and negative regulation of IkappaB kinase activity through IKKbeta subunit phosphorylation. *Science.* 1999; 284:309–13. [PubMed: 10195894]
22. Johnson LN, Noble ME, Owen DJ. Active and inactive protein kinases: structural basis for regulation. *Cell.* 1996; 85:149–58. [PubMed: 8612268]
23. Shin HM, Kim MH, Kim BH, et al. Inhibitor action of novel aromatic diamine compound on lipopolysaccharide-induced nuclear translocation of NF-kappaB without effecting IkappaB degradation. *FEBS Lett.* 204(571):50–54.

24. Seol W, Choi HS, Moore DD. An orphan nuclear hormone receptor that lacks a DNA binding domain and heterodimerizes with other receptors. *Science*. 1996; 272:1336–1339. [PubMed: 8650544]
25. Choi YH, Park MJ, Kim KW, Lee HC, Choi YH, Cheong J. The orphan nuclear receptor SHP is involved in monocytic differentiation and its expression is increased by c-Jun. *J Leukoc Biol*. 2004; 76:1082–1088. [PubMed: 15292277]
26. Zhang Y, Dawson MI, Mohammad R, et al. Induction of apoptosis of human B-CLL and ALL cells by a novel retinoid and its nonretinoidal analog. *Blood*. 2002; 100:2917–2925. [PubMed: 12351403]
27. Ortiz MA, Lopez-Hernandez FJ, Bayon Y, Pfahl M, Piedrafita FJ. Retinoid-related molecules induce cytochrome c release and apoptosis through activation of c-JunH<sub>2</sub>-terminal kinase/p38 mitogen activated protein kinases. *Cancer Res*. 2001; 61:8504–12. [PubMed: 11731435]
28. Holmes WF, Soprano DR, Soprano KJ. Early events in the induction of apoptosis in ovarian carcinoma cells by CD437 activation of the p38 MAPP kinase signal pathway. *Oncogene*. 2003; 22:6377–86. [PubMed: 14508518]
29. Jin F, Liu X, Zhou Z, et al. Activation of nuclear factor-kappaB contributes to induction of death receptors and apoptosis by the synthetic retinoid CD437 in DU145 human prostate cancer cells. *Cancer Res*. 2005; 65:6354–63. [PubMed: 16024638]
30. Kim HJ, Hawke N, Baldwin AS. NF-κB and IKK as the therapeutic targets in cancer. *Cell Death Differ*. 2006; 13:238–47.
31. Pfahl M, Piedrafita FJ. Retinoid targets for apoptosis induction. *Oncogene*. 2003; 22:9058–9062. [PubMed: 14663484]
32. Kim Y-S, Han C-Y, Kim S-W, et al. The orphan nuclear receptor small heterodimer partner as a coregulator of nuclear factor-κB in oxidized low density lipoprotein-treated macrophage cell line RAW 264.7. *J Biol Chem*. 2001; 276:33736–33740. [PubMed: 11448950]
33. Nishizawa H, Yamagata K, Shimomura I, et al. Small heterodimer partner, an orphan nuclear receptor, augments peroxisome proliferators-activated receptor γ transactivation. *J Biol Chem*. 2002; 277:1586–1592. [PubMed: 11696534]
34. He N, Park K, Zhang Y, Huang J, Lu S, Wang L. Epigenetic inhibition of nuclear receptor small heterodimer partner is associated with and regulates hepatocellular carcinoma growth. *Gastroenterology*. 2008; 134:793–802. [PubMed: 18325392]
35. Zhang Y, Xu P, Park K, Choi Y, Moore DD, Wang L. Orphan receptor small Heterodimer partner suppresses tumorigenesis by modulating cyclin D1 expression and cellular proliferation. *Hepatology*. 2008; 48:289–298. [PubMed: 18537191]
36. Bruserud Ø, Rynningen A, Olsnes AM, et al. Subclassification of patients with acute myelogenous leukemia based on chemokine responsiveness and constitutive chemokine release by their leukemic cells. *Haematologica*. 2007; 92:332–341.
37. Cowley SM, Kang RS, Frangioni JV, et al. Functional analysis of the Mad1-Sin3A repressor-corepressor interaction reveals determinants of specificity, affinity and transcriptional response. *Mol Cell Biol*. 2004; 24:2698–2709. [PubMed: 15024060]
38. Shiiro Y, Rose DW, Aur R, Donohoe S, Aebersold R, Eisenman RN. Identification and characterization of SAP25, a novel component of the Sin3 repressor complex. *Mol Cell Biol*. 2006; 26:1386–1397. [PubMed: 16449650]
39. Zhang Y, Itratni R, Erdjument-Bromage H, Tempst P, Reinberg D. Histone deacetylases and SAP18, a novel polypeptide are components of a human Sin3 complex. *Cell*. 1997; 89:357–364. [PubMed: 9150135]
40. Ayer DE, Lawrence QA, Eisenman RN. Mad-Max transcriptional repression is mediated by tertiary complex formation with homologs of yeast repressor Sin3. *Cell*. 1995; 80:777–786. [PubMed: 7889571]



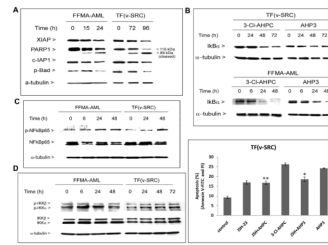
**Figure 1.**

Apoptosis induction in FFMA-AML and TF(v-SRC) cells by 3-Cl-AHPC and AHP3. (A) Structures of 3-Cl-AHPC and AHP3. (B) Cells were seeded at  $1 \times 10^4$  cells/ml and grown for 24 h, then exposed to varying concentrations of AHP3 or 3-Cl-AHPC for 96 h, (C) incubated with AHP3 or 3-Cl-AHPC ( $1 \mu\text{M}$ ) for 0 to 96 hours and (D) exposed to  $1 \mu\text{M}$  all trans retinoic acid, 9-cis-retinoic acid and TTPNB. The percentage of apoptotic cells was determined using acridine orange and ethidium bromide staining as described in Materials and Methods. The error bars represent the mean of three separate determinations  $\pm$  the standard deviation (SD).



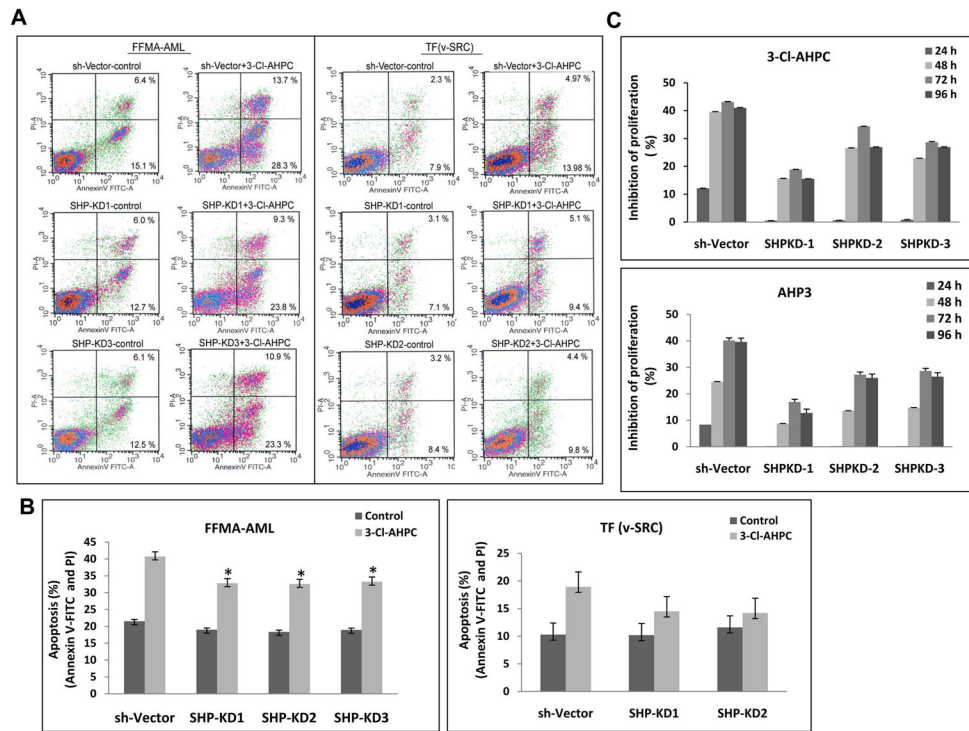
**Figure 2.**

Induction of apoptosis and 3-Cl-AHPC and AHP3 mediated caspase-3 activation and cleavage of caspase-3. FFMA-AML and TF(v-SRC) cells were exposed to 1  $\mu$ M 3-Cl-AHPC and AHP3. (A) Apoptosis in FFMA-AML and TF(v-SRC) cells following 24 and 48 h ARR exposure, respectively. (B) Percentage of apoptotic cells for indicated times. Induction of apoptosis and cell death was assessed using Annexin V-FITC labeling with propidium iodide (PI) staining; the percentage of apoptotic cells corresponds to the sum of percent noted in upper right (late apoptotic cells, annexin V and PI positive cells) and lower right (early apoptotic cells, annexin V positive, PI negative) quadrants. (C) Activation of caspase-3 in FFMA-AML and TF(v-SRC) cells following exposure to ARR for varying times. (D) Generation of caspase -3 (17 kDa) fragment and caspase-3 protein levels. Caspase-3 activation was determined as described in Methods. The error bars represent the mean of three separate determinations  $\pm$  the standard deviation. \*, \*\* and \*\*\* were significantly different in comparison to control cells. ( $p$  value is  $<0.05$ ,  $<0.01$  and  $<0.001$  as determined by  $t$  test).



**Figure 3.**

AHP3-mediated inhibition XIAP, c-IAP1, and phospho-Bad expression in FFMA-AML and TF(v-SRC) cells accompanied by the induction of PARP cleavage, AHP3 and 3-Cl-AHPC induce NF- $\kappa$ B activation in canonical pathway. (A) AHP3 decreased the expression of XIAP, c-IAP1 and phospho-Bad protein in Western blot. (B) AHP3 and 3-Cl-AHPC enhanced the I $\kappa$ B $\alpha$  degradation, and (C) NF- $\kappa$ Bp65(Ser276) phosphorylation in AML cells. (D) 3-Cl-AHPC enhanced IKK $\alpha$  (Ser180) and IKK $\beta$  (Ser181) phosphorylation/activation in cells (left panel). NF- $\kappa$ B inhibitor, JSH-23 inhibited ARR mediated apoptosis in TF(v-SRC) cells (right panel); cells were treated for 48 h. \* and \*\* significantly different in comparison to control cells ( $p$  value is  $<0.05$  and  $<.01$  as determined by  $t$  test). The error bars represent the mean of three separate determinations  $\pm$  the standard deviation.

**Figure 4.**

Loss of SHP expression inhibited 3-Cl-AHPC-induced apoptosis and in AML cells. (A and B) Knockdown of SHP expression inhibited 3-Cl-AHPC mediated apoptosis in FFMA-AML and TF(v-SRC) cells. FFMA-AML and TF(v-SRC) cells were transfected with shRNA SHP retroviral expression vectors for 48 h, then cells were exposed to 1  $\mu$ M 3-Cl-AHPC for 15 and 24 h, respectively. Apoptosis was assessed by flow cytometry using Annexin V-FITC and propidium iodide. (C) SHP knockdown blocked the 3-Cl-AHPC and AHP3 mediated inhibition of proliferation in TF(vSRC) cells. The error bars represent the mean of three separate determinations  $\pm$  the standard deviation. \* significantly different in comparison to sh-vector treated cells ( $p$  value is  $<0.05$  as determined by  $t$  test).

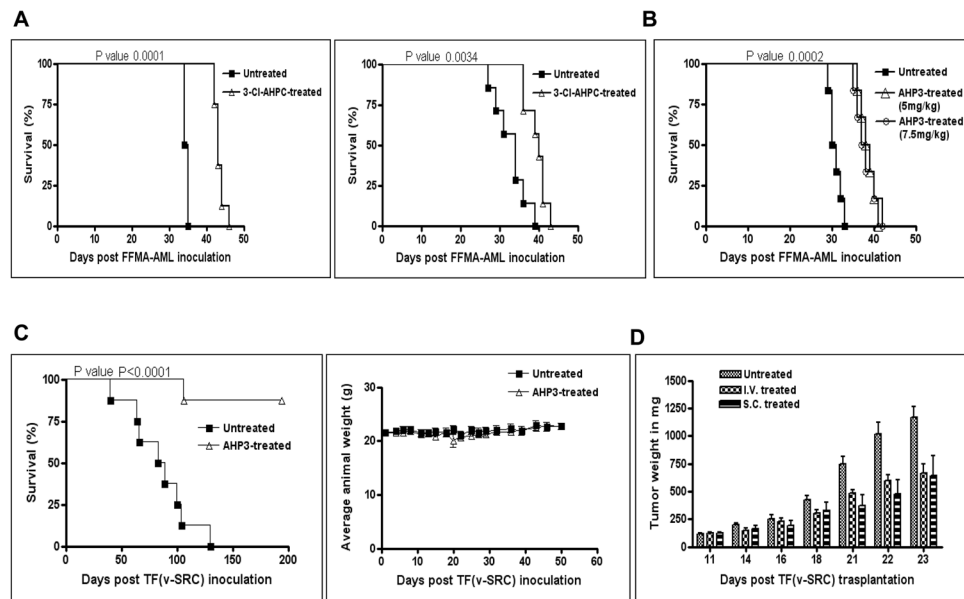


**Figure 5.**

AHP3 and 3-Cl-AHPC inhibition of FFMA-AML proliferation in NOD-SCID mice, prolongation of survival and AHP3 inhibited TF(v-SRC) proliferation and growth in SCID mice. (A) Sixteen NOD-SCID mice were randomly divided into two groups of eight mice each and were injected through the tail vein with  $1 \times 10^6$  FFMA-AML cells. Treatment with either vehicle or 3-Cl-AHPC (30 mg/kg) given twice intravenously daily for 4 days was instituted 24 h following injection of the cells (left panel). An second study, identical to the one described above, was performed with 3-Cl-AHPC by an interperitoneal route (A, right panel). (B) Twenty four NOD-SCID mice were randomly divided into three groups of eight mice each. Each mouse was injected with  $1 \times 10^6$  FFMA-AML cells; 24 h later after injection, treatment was started with either vehicle or AHP3 given at doses 7.5 mg/kg or 5.0 mg/kg intravenously twice daily through the tail veins for 5 days. Mice were then observed daily for evidence of toxicity and prolongation of survival time. (C) Survival of TF(v-SRC) inoculated mice treated with AHP3. NOD SCID mice were randomly divided into two groups of eight mice. Each mouse was injected with  $1 \times 10^7$  TF(v-SRC) cells and 24 h later mice were either treated intravenously with AHP3, 20 mg/kg or vehicle on a Monday, Wednesday and Friday schedule for a total of 15 injections. Mice were observed daily for evidence of toxicity and prolongation of survival. Absence of weight loss in AHP3 treated SCID mice (C, right panel). (D) AHP3 inhibited palpable TF(v-SRC) growth in SCID mice. TF(v-SRC) cells were grown and maintained subcutaneously in a SCID mouse. Tumors were harvested and approximately 20 mg of tumor was subcutaneously trochared into each flank of a SCID mouse. The tumors were then allowed to reach a size of 100 mg and the mice randomly divided into three groups of 8. Groups were administered 20 mg/kg AHP3 either intravenously (I.V.) or subcutaneously (S.C.) (at a site distant from the tumor) on a Monday, Wednesday and Friday scheduled for 12 injections. Control mice were treated intravenously with vehicle. The error bars represent the standard deviation.



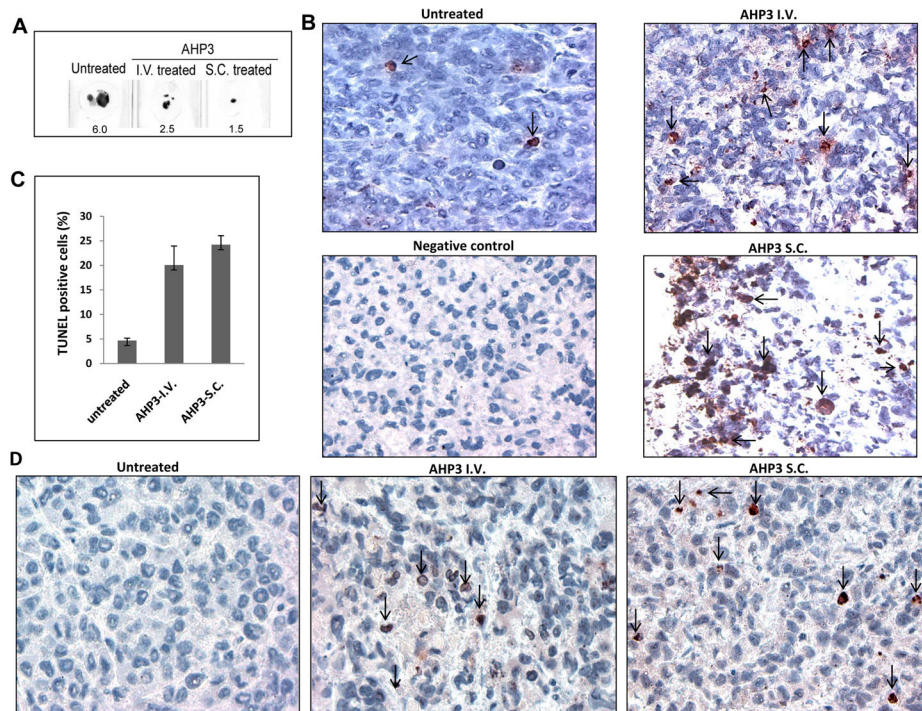


**Figure 6.**

AHP3 mediated apoptosis and PARP cleavage in treated tumor tissues. (A) Size of untreated and AHP3 treated paraffin embedded tumor tissue sections in millimeter. (B) DNA strand breaks in tumors obtained from vehicle and AHP3 intravenously (I.V.) or subcutaneously (S.C.) treated mice were detected by TUNEL assay using the *in situ* detection kit. (C) TUNEL positive cells in tumor tissues. (D) Immunohistochemical staining of paraffin-embedded tissue sections for cleaved PARP. Apoptotic cells were indicated by arrow. Details of slides preparation, visualization and antibody utilized are described in Materials and Methods.